X-ray photoelectron diffraction study of the approximant Al5Co2(001) quasicrystal

Lhonidas de Senna Junior, Alexandre Pancotti, Alex Sandre Kilian, Abner de Siervo, Renee Diehl, Marie-Cécile de Weerd, Julian Ledieu, Émilie Gaudry, Vincent Fournée, Guilherme Jean P. Abreu

X-ray photoelectron diffraction study of the approximant Al_5Co_2(001) quasicrystal

Lhonidas de Senna Junior[1], Alexandre Pancotti[2], Alex Sandre Kilian[2], Abner de Siervo[3], Renee D. Diehl[4], Marie-Cécile de Weerd[5], Julian Ledieu[5], Emilie Gaudry[5], Vincent Fournée[5], and Guilherme Jean P. Abreu[1]

[1]Departamento de Física, Universidade Federal do Paraná- Curitiba Brazil
[2]Departamento de Física, Universidade Federal de Jataí – Jataí, Brazil
[3]Departamento de Física Aplicada, Instituto de Física Gleb Wataghin, Universidade Estadual de Campinas
[4]Department of Physics, Penn State University, University Park, Pennsylvania 16802, USA
[5]Institut Jean Lamour, UMR CNRS 7198, Université de Lorraine, 54011 Nancy cedex, France

Abstract

The intermetallic Al_5Co_2 is defined as a structurally complex material and is considered a low-order quasicrystalline approximant. A single crystal of Al_5Co_2(001) was obtained by the Czochralski method. The sample was characterized by X-ray photoelectron spectroscopy (XPS), low-energy electron diffraction (LEED), and X-ray photoelectron diffraction (PED). The surface composition was also analyzed by XPS, indicating only Al and Co compounds. In the current research, the crystal structure was qualitatively analyzed by the LEED patterns for different incident beam energies indicating a (1×1) termination, also in accordance with some literature works. The structure study was performed applying the standard software MSCD and show a (1×1) pattern. In addition, four different termination models for this termination were tested. The reliability factor indicated the best termination belongs to the Al-rich surface layer.

Introduction

Surface science studies about different materials show an increasing interest in industries and basic research. One of the most exciting material examples nowadays is the quasicrystals. These materials present an ordered, but not periodic in 3D structure, and in addition, they can present rotational symmetry of order 5, 8, 10, or 12; corresponding to a high degree of complexity and prohibited conditions to be considered as crystals (the definition of a crystal has been updated in 1992 to include quasicrystals). They present high hardness, low friction coefficient, low surface adhesion energy, and resistance to oxidation and corrosion[1].

Materials that have a combination of two or more metals in their alloy and a well-defined stoichiometry, as well as a completely or at least partly ordered crystal structure that differs from the structure of the main constituents, are called intermetallics. A general example would be aluminum–cobalt (Al–Co), which despite being an alloy studied for a long time, there are still difficulties in determining its structure, especially for Al-rich phases[2,5]. This difficulty is due to the complex metallic alloy, such as the compounds $Al_{13}TM_4$ (*TM* = Co or Fe) known as an approximation of the quasicrystals. These Al-rich cobalt aluminides (intermetallic compounds based on aluminum with transition metals) are interesting for high-temperature applications as they have a combination of high melting points, good corrosion resistance[2], and are a good candidate for catalytic purposes[5].

First observed in 1908 by Gwyer[4-8], the compound Al_5Co_2 belongs to the oldest known intermetallic phases and is rich in Al. Approximately 30 years later, Bradley and Cheng[6] investigated the structure of the compound using Debye-Scherrer X-ray photographs (using FeKα radiation). In this study, the Al_5Co_2 phase was identified in the compositional range of $Al_{0.711–0.720}Co_{0.289–0.280}$, forming by peritectic reaction of AlCo and melting point at 1455 K (1181 ºC)[6,7]. This investigation of the structure of Al_5Co_2 resulted in a Pearson symbol hP28, space group $P6_3/mmc$, a = b = 7.671(5) Å, c = 7.608(5) Å and c/a = 0.9918[6,7]. The Al_5Co_2 intermetallic can be considered as a small size approximant of decagonal quasicrystals. Its unit cell contains 28 atoms, thus relatively small compared to other Al–TM (*TM* = Transition Metal = Co, Fe or Ru) approximants, like the well-known $Al_{13}TM_4$ with 102 atoms per unit cell[2,5]. Its atomic structure resembles that of decagonal phases, with rotational symmetry of order 10, with local pentagonal atomic configurations. Belonging to the $P6_3/mmc$ space group with lattice parameters a = b = 7.671 A, c = 7.605 Å and hexagonal crystal system, as illustrated in Figure 1[5].

The structure in the (100) direction of the Al_5Co_2 compound consists of a periodic stacking of alternating atomic layers, puckered layers (P) having 7 Al atoms per layer, between Al_1 and Al_3 atoms, and flat layers (F) having 3 Al atoms and 4 Co atoms, between Co_1, Co_2, and Al_2. Stacked in a P1F2P2F1 array so that P1 and P2, or F1 and F2, are related by a rotation of 180º [5]. Meier *et al.,* (2015)[5] observed in their work three possibilities for surface terminations that depend only on the annealing temperature, namely a (2×2) termination for 823 K, a $(\sqrt{3}\times\sqrt{3})R30^o$ termination for 973 K, and a (1×1) termination for 1180 K.

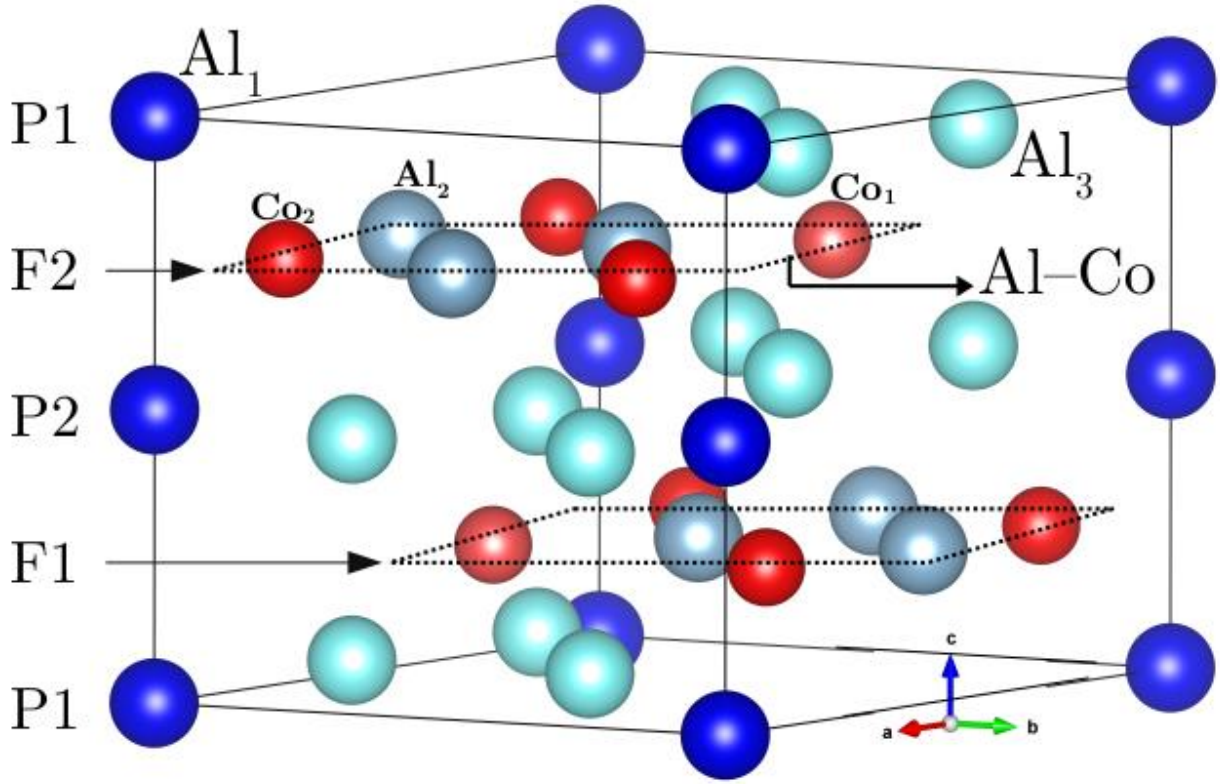

Figure 1: Hexagonal crystal structure of the compound Al_5Co_2 with blue atoms corresponding to Al and red ones to Co. The different shades of blue correspond to the different orders of Al by layer. We call Al–Co, the layer that contains the atoms Al_2, Co_1 and Co_2; We indicate the puckered layers (P) between the atoms of Al_1 and Al_3 and the flat layers (F) between Co_1, Co_2 and Al_2. Adapted from [5].

In order to better understand the intermetallic surface structures, we concentrated on the intermetallic compound Al_5Co_2, which is a good candidate for heterogeneous catalysis[5,9] as well. The goal of this article was to study Al_5Co_2(001) using the Low Energy Electron Diffraction (LEED) and X-ray Photoelectron Diffraction (PED) techniques for structural determination with the aid of the multiple scattering calculation diffraction (MSCD) simulation, developed by Chen and Van Hove (1997)[10], being the first PED measurement for Al_5Co_2 considered as an approximant to decagonal quasicrystal. The experiments were carried out on the Planar Grating Monochromator (PGM) beamline of the Brazilian Synchrotron Light Laboratory (LNLS), using an Ultra High Vacuum (UHV) station[11].

Our LEED results showed a possible (1×1) termination for the Al_5Co_2 surface. The precision structural analysis was performed by comparing experimental data obtained by PED and theoretical data using MSCD simulation. Four different termination models for this termination were tested. The results indicate a (1×1) termination, with the best reliability factor (R_a) value of 0.182 belonging to the Al-rich surface layer as

a combination of two distinct models. The interlayer relaxations of topmost surface slabs show a significant displacement in comparison to bulk distances.

Experimental and Simulation Details

Synthesis of Al_5Co_2

Single crystal growth can be obtained from an Al-rich solution at a temperature below its peritectic transformation at 1426 K. The initial composition of the Al-rich solution was selected according to the phase diagram ($Al_{76}Co_{24}$)[5]. A homogeneous solution was first prepared by precisely weighing the metal parts to the desired composition and pre-melted under an Argon (Ar) atmosphere using an induction furnace. After that, the mass of pre-molten metal, called an ingot, was placed in an alumina crucible in the Czochralski furnace, initially evacuated at a pressure of 10^{-6} mbar and filled with 700 mbar of Ar. A small single crystal with undefined orientation was used as a seed. This was placed in contact with the liquid solution, pre-molten metal, at a temperature of 1400 – 1426 K (1126.85 – 1152.85 ºC) and then pulled at a rate of 2 mm/h. This resulted in the growth of a single crystal several cm long and about 1 cm in diameter. Using the Laue back-reflection method, a sample Al_5Co_2 with (001) orientation was extracted from the crystal. The sample was then polished with a final polishing cycle using diamond paste of 0.25 µm. The chemical composition of the Al_5Co_2 compound was studied using the X-ray Photoelectron Spectroscopy (XPS) presented in a previously work by Meier *et al.,* (2015)[5].

Surface Characterization

The experiments were performed using the U11 beamline, the planar grid monochromator (PGM) of the Brazilian Synchrotron Light Laboratory (LNLS)[11] in a UHV system (base pressure 2×10^{-10} mbar) equipped with a high-resolution hemispherical electron analyzer (Omicron HA125HR with multi-channeltron detection) mounted in the plane of the storage electron ring, a LEED optics, a differentially pumped argon ion sputter gun for in situ sample cleaning and a five-axis (x, y, z, θ and φ) sample manipulator equipped for heating samples up to ~1600 K by electron bombardment[12]. The sample temperature was measured by an infrared pyrometer IMPAC 140 (573 – 1473 K).

The surface of an Al5Co2(001) crystal disk of 5 mm diameter and 2 mm thickness was prepared by several cycles of Ar sputtering (1.5 keV, for 30 minutes at room temperature) and annealing (from 933 K for 1 hour, 973 K for 1 hour, 1173 K for 1 hour and 2 cycles at 1173 K for 1 hour each) with the temperature monitored by an infrared pyrometer, until no trace of surface contamination could be observed in the photoemission spectrum and a high-quality LEED pattern with sharp diffraction spots and very low diffuse background was obtained.

The PED data were collected in angular scan mode. The azimuthal angle (φ) was varied in steps of 3º in an interval of 180º. This range was sufficient to observe all structures, and dataset replication was used only to obtain 360º azimuthal scans and allow a better graphical representation of the PED patterns. The polar angle (θ), defined as the angle between the analyzer axis and the normal to the surface, was varied in steps of 3º from 9º to 69º. The incoming photons from the PGM beamline at the LNLS had an energy of 350 eV. The photoemission lines measured were the Al 2p and Co 3p shake up satellite. However, for the main peak of Al, no diffraction was observed, while for the satellite of Co3p, yes. Despite not being common to use the satellite peak for this type of experiment, we decided to proceed with these results analysis. This analysis may be useful for opening new possibilities in the study of metallic alloys composed of many elements. This is because while many main peaks in these cases may an overlap, the satellite peaks increase the chances of having isolated peaks that are able to be acquired. Thus, the Co 3p satellite photoelectrons were emitted with 281 eV kinetic energy making them very surface sensitive.

Therefore, in the current investigation, for the first time, a satellite peak was chosen for the convenience of the experiments as well as to have almost the same kinetic energies for both emitting elements (Al and Co) in order to probe similar sample thickness for the structure determination.

The PED simulations were performed in a parallel cluster with forty processors, using the MSCD code (Chen and Van Hove[10]), where the calculations are performed for a cluster model with a parabolic format (radius of 13 Å and depth of 11 Å) containing approximately 310 atoms. The determination of the surface structure is performed by comparing the experimental and simulated diffraction patterns through the relaxation of structural parameters (interlayer distances, lattice parameters, etc.) and non-structural (internal potential and Debye temperature). Automated structure optimization is based on a genetic algorithm implemented in MSCD code by Viana *et*

al., (2007)[13,] and the quality of agreement is evaluated by the known reliability factor R_a defined by:

$$R_a = \sum_i \frac{\left(\chi_c^i - \chi_e^i\right)^2}{\left(\chi_c^i\right)^2 + \left(\chi_e^i\right)^2},$$

where χ_c^i and χ_e^i correspond to the calculated and experimental curves, respectively. The closer to zero R_a is the better the agreement with the experiment[12-21].

As a measure of the quality of the R-factor, the uncertainties can be calculated using the steepness of the R-factor space assigned to a parameter in the vicinity of its absolute minimum and the maximum number of separable diffraction information N with an experimental data:

$$Var(R_{min}) = R_{min}\sqrt{2/N},$$

with $Var(R_{min})$ being the variance of R at the minimum[12-21]. This way of calculating uncertainty was used by Van Hove *et al.,* (1993)[22].

The photoemission intensities from different polar and azimuthal angles are normalized by the function χ, presented in the form of an anisotropy, given by:

$$\chi\left(\theta,\varphi,\vec{k}\right) = \frac{I\left(\theta,\varphi,\vec{k}\right) - I_0\left(\theta,\varphi,\vec{k}\right)}{I_0\left(\theta,\varphi,\vec{k}\right)},$$

where $I\left(\theta,\varphi,\vec{k}\right)$ is the measured or calculated photoemission intensity over all angles φ for a given angle θ, representing the background in the experiment and $I_0\left(\theta,\varphi,\vec{k}\right)$ is the photoelectron intensity in the absence of diffraction (free atom)[12-22].

Results and Discussion

The surface termination analysis was performed using LEED results, for 5 different energies of the incident beam after annealing, being 34 eV, 50 eV, 80 eV, 103 eV and 150 eV, respectively, as shown in Figure 2. The Al_5Co_2 (001) layers are stacked in a P1F1P2F2 arrangement such that P1 and P2, or F1 and F2, are related by a rotation of 180º. There are also other symmetry operations linking the P1 and P2 / F1 and F2 planes. However, each of the two ruffled terminations would produce a diffraction pattern with three-fold symmetry, and a surface with half of each termination (P1 + P2 or F1 + F2) would produce a diffraction pattern with six-fold symmetry, as seen in Figure 2.

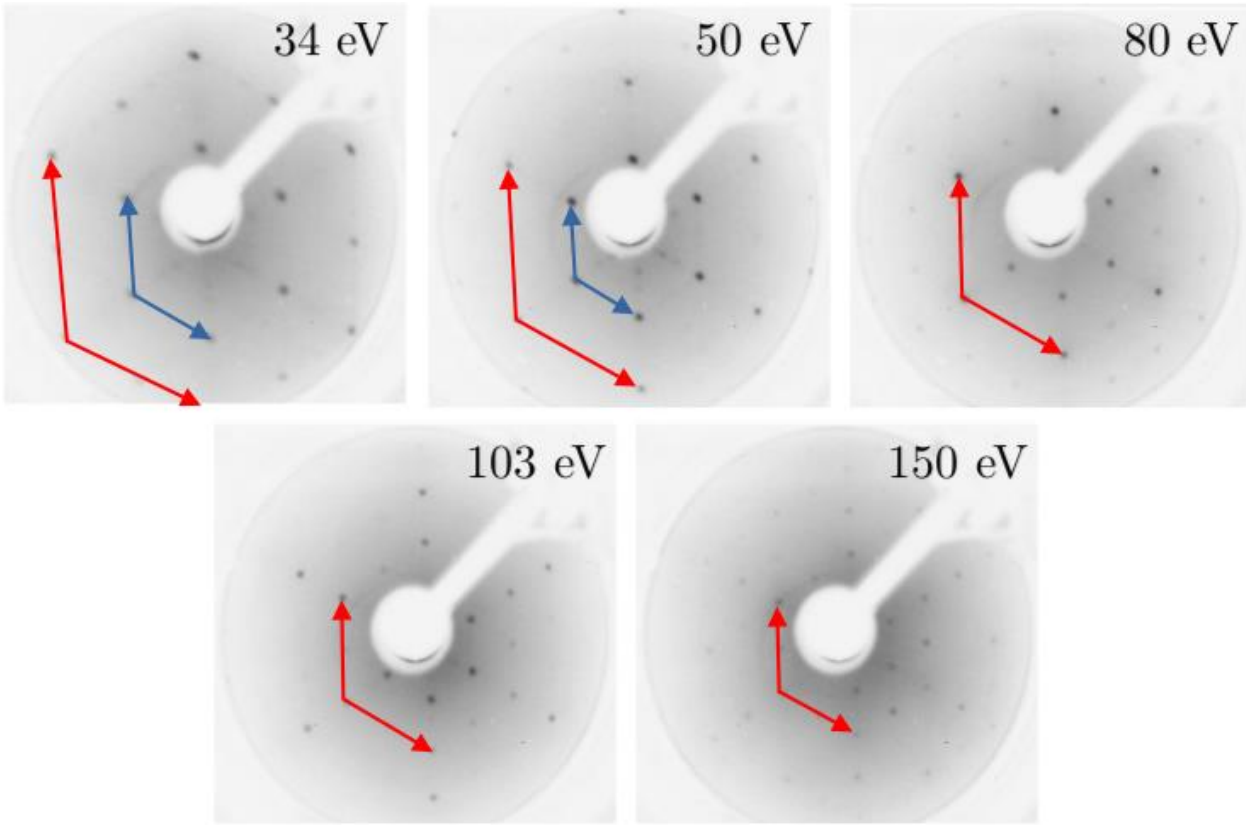

Figure 2: LEED patterns obtained for the energies of 34, 50, 80, 103 and 150 eV for the study of the surface of the Al_5Co_2 (001) compound.

We obtained a well-defined LEED pattern across the entire range. Indicating good ordering of the sample surface. Therefore, based on the pattern information and previous information from the literature, we can deduce the termination that would be compatible with this surface should be the (1×1) [5]. Then, we performed the PED measurement and the MSCD construction for the proposed terminations.

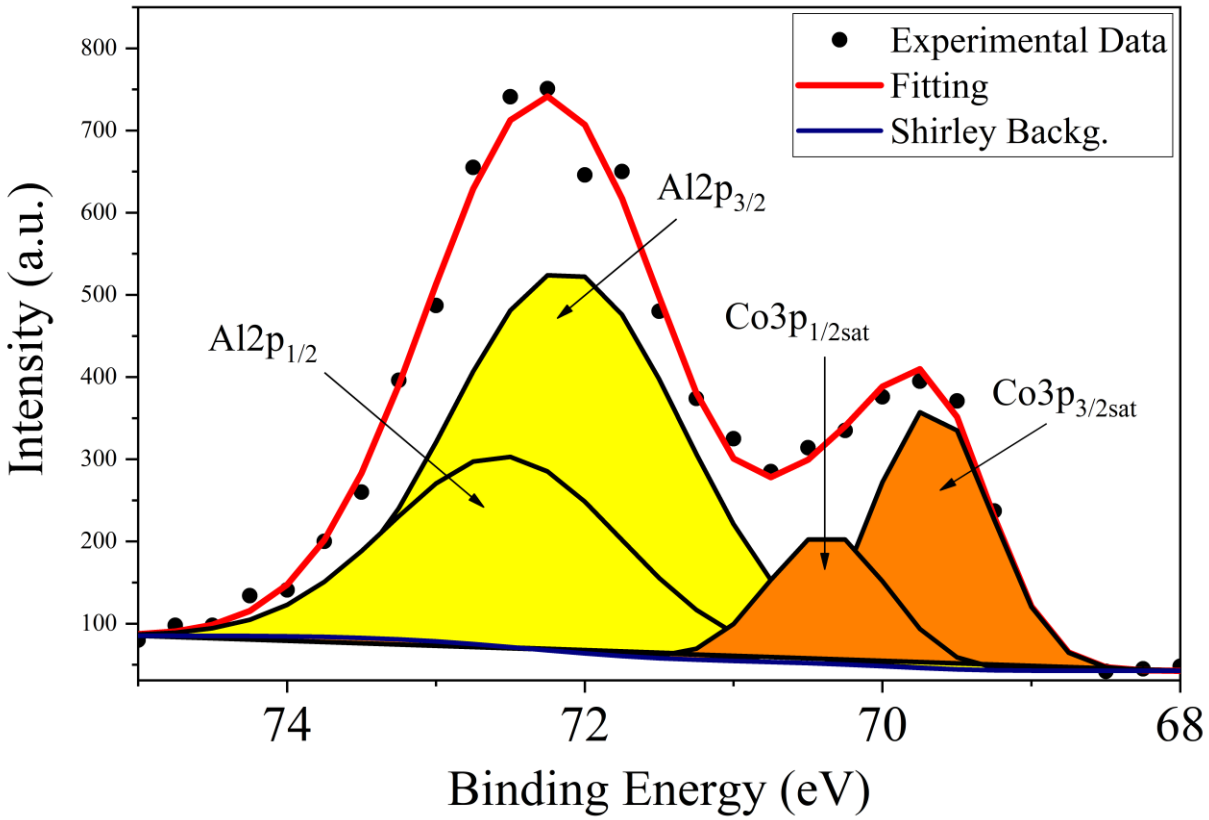

Figure 3: Representation of an Al_5Co_2 XPS spectrum through PED data, containing information on the levels of the Al 2p core with the $2p_{3/2}$ and $2p_{1/2}$ components represented by the color yellow and for the Co 3p satellite with the $3p_{3/2}$ and $3p_{1/2}$ represented by the color orange.

The PED acquisition was performed in a small range between 68 eV and 75 eV. The peaks deconvolution was accomplished as illustrated in Figure 3. It is possible to notice that in the XPS result there is the contribution of Al 2p and also of the Co 3p satellite (Figure 3). This observation coincides with the result reported by Verdier *et al.,* (2007)[23], who obtained the same peaks with very close binding energies. For Al they reported $2p_{3/2}$ and $2p_{1/2}$ at 73.3 eV and 74.3 eV, respectively, and for the Co satellite, they reported $3p_{3/2}$ and $3p_{1/2}$ at 69.3 eV and 71.3 eV, respectively[23]. The shift of Co satellite peak in binding energy relative to the Co 3p core peak is 9.5 eV.

According to the work of Frost *et al.,* (1974)[24] we can say that the satellite peak of Co 3p (Figure 3) is of the shake-up type. This corresponds to a multielectron process denominated shake-up state. In this process part of the photon energy is used in the one-step process to promote another electron into an unoccupied state and the photoelectron is consequently emitted with lower kinetic energy[24].

According to the PED patterns of $Al2p_{3/2}$ and $Co3p_{3/2}$ satellite and their anisotropies, it was possible to notice that the Co pattern was the best diffracted with

56% anisotropy, while Al resulted in 8%. So, we decided to work with the Co $3p_{3/2}$ satellite pattern, since for Al we didn't get a “clear” pattern. We believe that it is the response of an Al-rich surface, thus causing overlapping intensities. The MSCD inputs have wide information set like radial scattering matrices (corresponds to the probability of photoelectron transition within the atom from bound to continuous state), phase differences (related to the way the electron scatters in the crystal), and the PED experimental data, according to the X-ray beam energy of 350 eV. We consider Co atoms as the emitters, that is, those responsible for initiating the multiple scattering process within the material and thus resulting in a PED pattern. The initial simulation condition was the same presented in the previous work Meier *et al.,* (2015)[5], with its structure file CIFICSD_CollCode109470 used for the atomic positions of each atom and the distances between the physical layers. Its unit cell is represented in Figure 1.

In the current work the model tested was a (1×1) surface termination using four different models for the analysis of the experimental data. These models are shown in Figure 4.

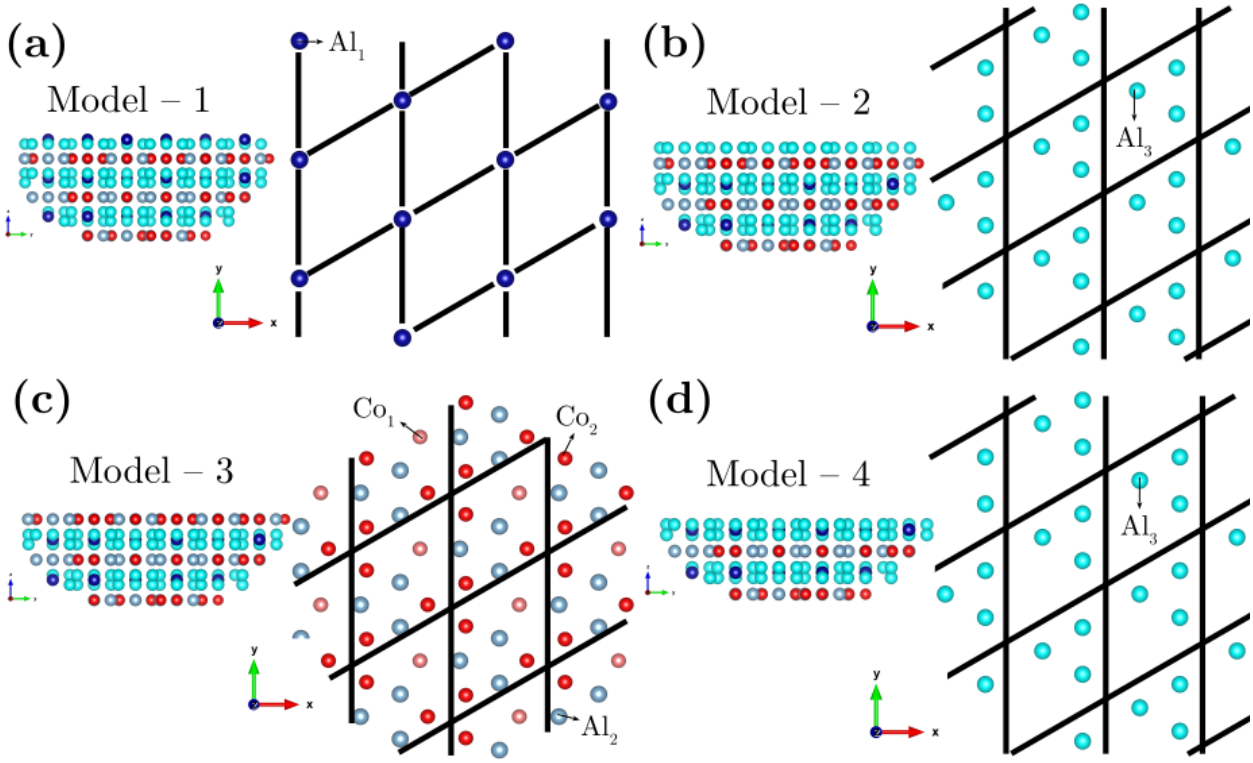

Figure 4: Representation of the 4 cluster models in orientation [001]. The blue and red spheres correspond to Al and Co atoms, respectively.

The initial lattice parameter was 7.656 Å, however, we decided to perform the optimization of this for model – 1 (Meier model[5]), to see whether there would be any change in this parameter value, consequently, the decrease or increase in the value of R_a. The best value was R_a = 0.421, corresponds to our new surface lattice parameter of 7.625 Å for the four different termination models.

In sequence, we performed the optimization of 5 first distances between physical layers, for each model, including a sixfold symmetry. The results of this simulation are presented in Figure 5. The optimization results indicated that the Al_5Co_2 (001) surface consists of alternating P1 and P2 layers, and both are related by an 180° rotation. This is why the surface appears 6-fold, while each terrace is 3-fold, thus explaining the pattern of 6 points of intensities in the LEED shown in the Figure 2.

The four distinct models are: model – 1 – This model present a bulk structure with termination in an Al_1 layer; model – 2 In this case we have the same structure presented in model – 1, but has taken out the first physical layer, i.e., and now it is terminated in an Al_3 layer; model – 3 In this model we have taken out the first and second physical layers in model – 1, and it present a termination in an Al and Co layer; model – 4 in this model we have taken out the first, second and third physical layers in the model – 1, i.e., so, we have a termination in the Al_3 layer. Notice the first layer in the model – 2 and model – 4 are the same, however, the next inner layers are different.

The optimized values for the distances of the five first physical layers of the Al_5Co_2(001) are represented in the tables (1 to 4) below for each model (1 to 4) respectively. We also place the values of the bulk structure (according to the unit cell in Figure 1) corresponding to each termination.

Table 1: Optimization results for the model – 1, containing the values of the bulk structure and the standard deviation between the data (σ).

Distance between Layers	**Bulk**	**Model – 1**	**σ**
d_{12}(Å)	0.451	0.937	±0.344
d_{23}(Å)	1.427	2.369	±0.667
d_{34}(Å)	1.427	1.556	±0.091

d_{45}(Å)	0.450	0.478	±0.019
d_{56}(Å)	0.451	0.745	±0.208
R_a	**0.492±0.034**	**0.352±0.014**	

Table 2: Optimization results for the model – 2, containing the values of the bulk structure and the standard deviation between the data (σ).

Distance between Layers	**Bulk**	**Model – 2**	**σ**
d_{12}(Å)	1.427	2.249	±0.582
d_{23}(Å)	1.427	1.426	±0.001
d_{34}(Å)	0.450	0.991	±0.382
d_{45}(Å)	0.451	0.198	±0.179
d_{56}(Å)	1.427	1.307	±0.085
R_a	**0.434±0.029**	**0.296±0.021**	

Table 3: Optimization results for the model – 3, containing the values of the bulk structure and the standard deviation between the data (σ).

Distance between Layers	**Bulk**	**Model – 3**	**σ**
d_{12}(Å)	1.427	1.664	±0.168
d_{23}(Å)	0.450	0.832	±0.270
d_{34}(Å)	0.451	0.772	±0.227
d_{45}(Å)	1.427	1.427	±0.000
d_{56}(Å)	1.427	1.427	±0.000
R_a	**0.535±0.013**	**0.463±0.010**	

Table 4: Optimization results for the model – 4, containing the values of the bulk structure and the standard deviation between the data (σ).

Distance between Layers	**Bulk**	**Model – 4**	**σ**

d_{12}(Å)	0.450	0.300	±0.106
d_{23}(Å)	0.451	0.451	±0.000
d_{34}(Å)	1.427	0.907	±0.367
d_{45}(Å)	1.427	1.592	±0.117
d_{56}(Å)	0.450	0.453	±0.002
R_a	**0.413±0.011**	**0.229±0.007**	

The theoretical PED pattern to model – 4, indicates an excellent agreement with the experimental data, strongly proving that we have in fact a (1×1) termination, and indicating a most likely termination as well. Both computational (as seen in Table 4) and even visual features (Figure 5) indicate the agreement between model – 4 and experimental data, having the best reliability factor, with R_a = 0.229. Also, model – 4 is also the only one that shows a contraction of d_{12}. This is in agreement with the results of the LEED-IV analysis of the "high-temperature" phase reported in presented in previous work Meier *et al.,* (2015)[5], corresponding to a (1x1) termination, proven by the direct comparison between Figure 2 and the Meier *et al.,* (2015)[5] patterns.

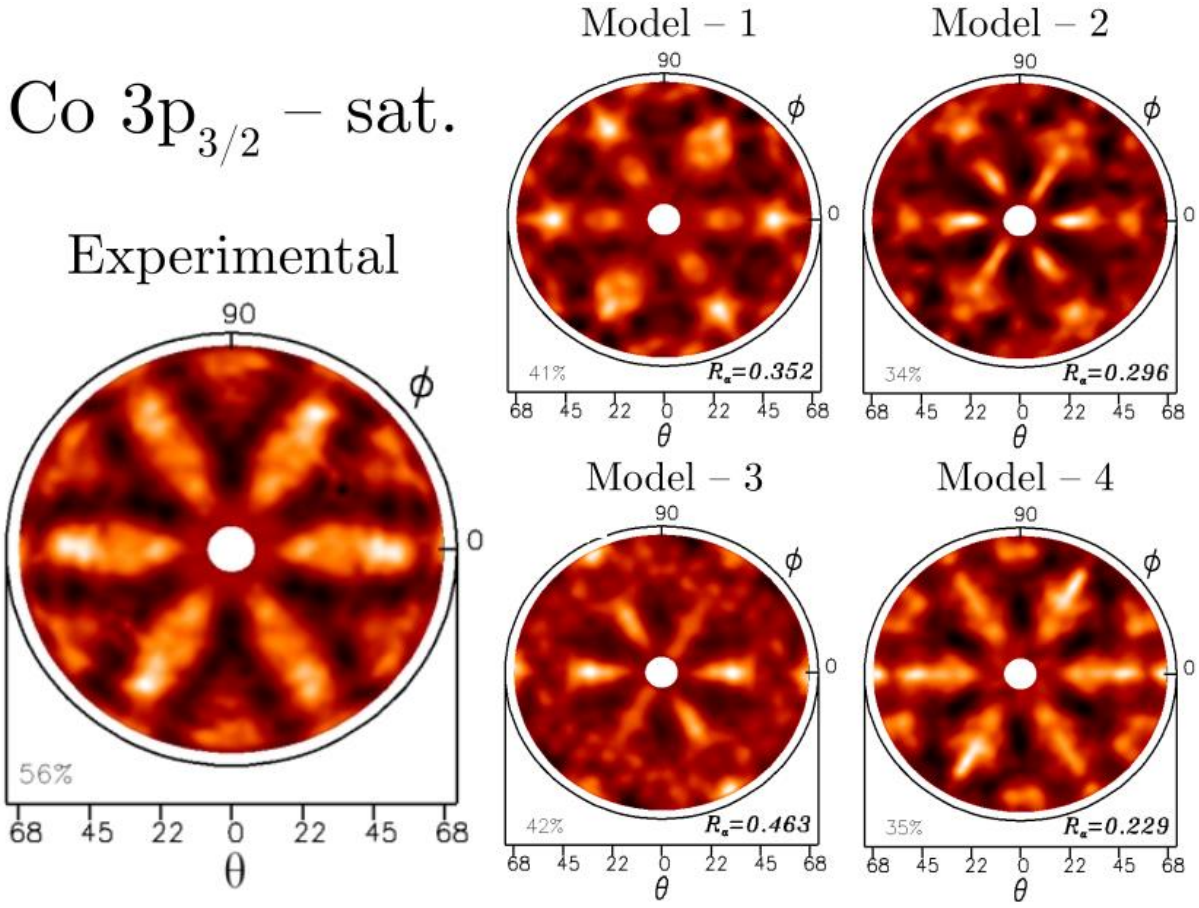

Figure 5: Photoelectron diffraction pattern of the Co $3p_{3/2}$ satellite, excited with 350 eV photons. On the left we have the experimental pattern and on the right the four optimized theoretical models.

The value shown at the bottom left of the photoelectron diffraction pattern, illustrated in Figure 5, refers to anisotropy. Model 2 and 4 have the lowest anisotropy values. The optimal model that does reproduce the minor entity of the modulations are the model 4 and 2. The anisotropy value for model 2 and model 4 are 34% and 35%. The models that present higher R_a values also present higher anisotropy values.

To further illustrate the agreement, we present in Figure 6 a comparison between theoretical curves, provided by the simulation, and experimental curves already optimized for each termination. We chose four different polar angles that were performed in the azimuthal range from 30º to 210º and considered with Co $3p_{3/2}$ emitting, that are shown in Figure 6. Figure 6-a (i to iv) shows the results to model 1 for the polar angles 27º, 36º, 48º e 63º, while the figure 6-b (i to iv), 6-c (i to iv) 6-d (i to iv) shows the same angles to models 2, model 3 and model 4, respectively. We note that for angle of θ = 63º, which bring more surface structural information, we obtain low-reliability factors.

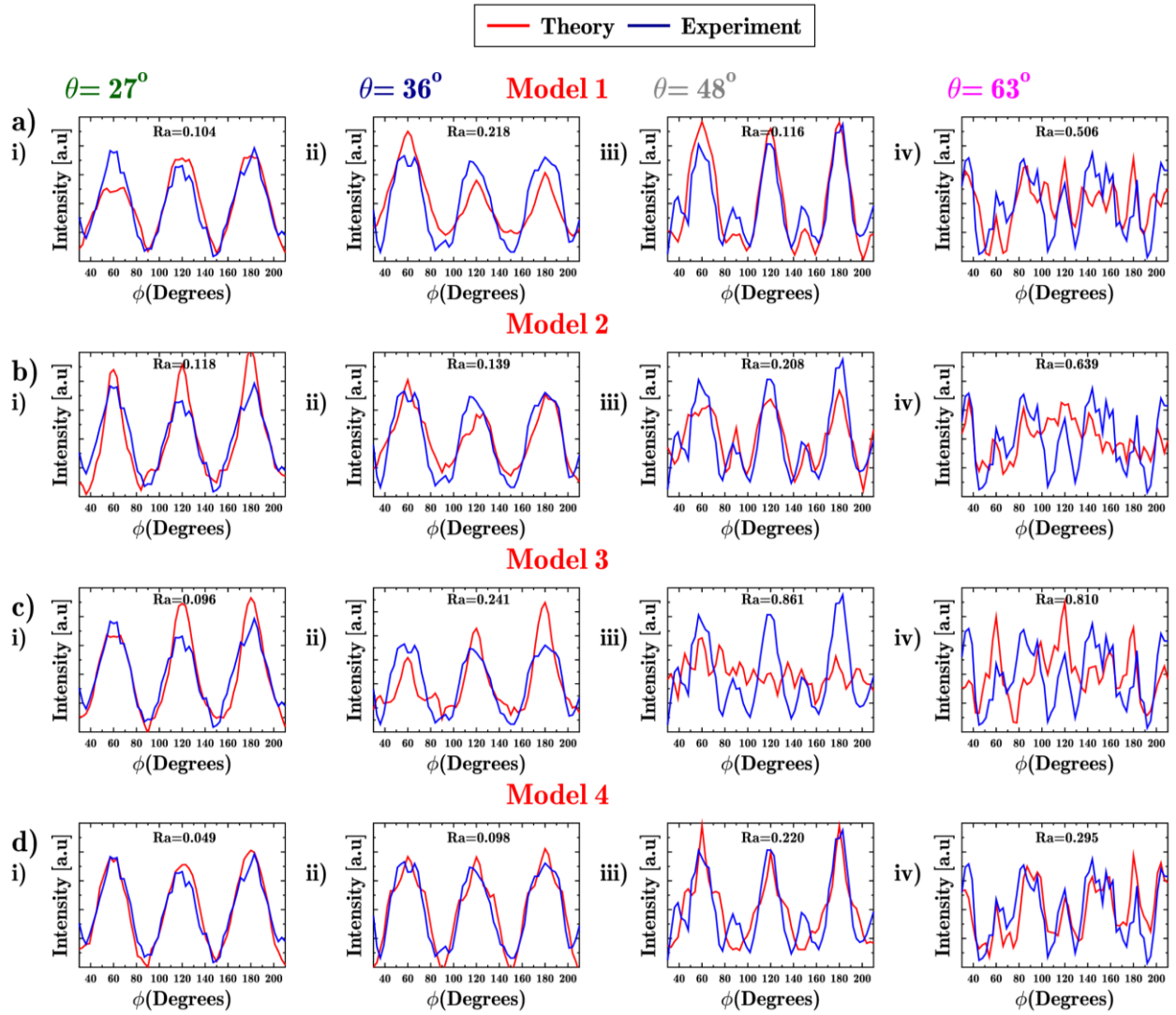

Figure 6: Comparison between simulation, performed using MSCD, and experimental data from PED for four different polar emission angles for Co $3p_{3/2}$ emitting with the 4 models. Red curves indicate MSCD simulation results and blue curves indicate experimental data.

The PED calculation uses several non-structural parameters, such as the Debye temperature (θ_D) and the internal potential (V_0). For Al_5Co_2(001) the temperature θ_D and V_0 were optimized, in relation to the model – 4, and presented a better R_a for θ_D = 575 K (Figure 7(a)) and V_0 = 4.6 eV (Figure 7 (b)). The value of θ_D = 575 K is close to the values found in literature[5], in which they obtained θ_D = 600 K through experimental data (obtained from the specific heat of the Al_5Co_2 compound with respect to heating) and θ_D = 550 K by calculations using the Debye model equation[5].

It is possible to notice, in Figures 4 and 5, that both model - 2 and model - 4 have terminations with the same type of Al_3 atoms of triangular geometry. Eventually, by linearly combining the models, the R_a factor can improve and, thus, the surface

will be formed by the superposition of the terminations of models 2 and 4. The linear combination is represented in Figure 7 (c).

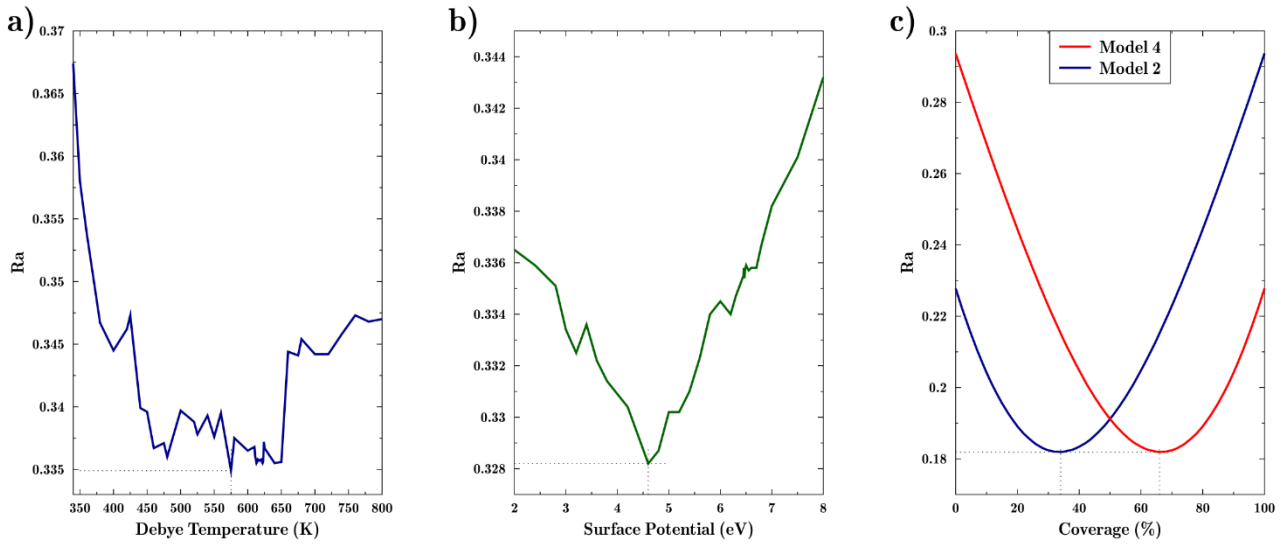

Figure 7: a) Result of R_a optimization as a function Debye Temperature; b) Result of R_a optimization as a function of surface potential (V_0) and the best value found was V_0 = 4.6 eV; c) Result of R_a as a function linear combination between models 2 and 4, in which the best value was for 66% of the model – 4 and 34% of the model – 2.

By inserting the new non-structural parameters, θ_D = 575 K and V_0 = 4.6 eV, we performed the construction of the PED pattern in relation to the result of the linear combination of the terminations of models 2 and 4, represented in Figure 7(c). This model is formed by 34% of model – 2 and 66% of model – 4, having an R_a = 0.182, this result is shown in Figure 8.

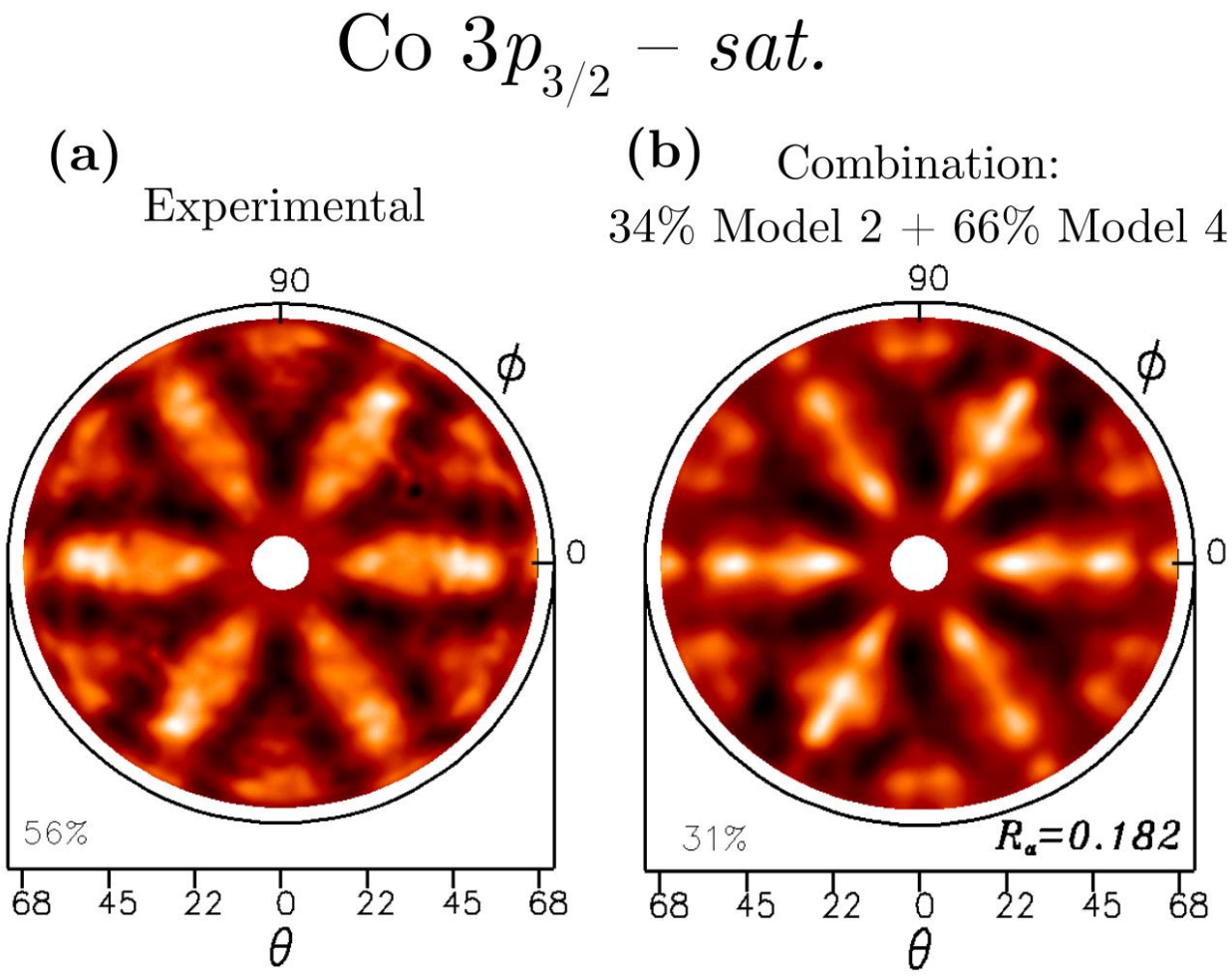

Figure 8: Comparison between the PED standards: (a) Experimental and (b) Theoretical corresponding to the linear combination of the terminations of models 2 and 4 and containing the parameters θ_D = 575 K and V_0 = 4.6 eV.

The model corresponding to the linear combination presented the best R_a result, thus further confirming the study by Alarcón *et al.,* (2011)[25], which states that in the case of the surface (001) for the Al_5Co_2 compound the Al-rich atomic layer is preferred as a surface termination rather than layers of mixed Al-Co[25]. Therefore, as the surface termination of Al_5Co_2(001) does not contain Co atoms, the catalytic reactivity of the surface-oriented in (001) is expected to be low, although the Co atoms below the surface slightly influence the electronic structure of the surface[26]. According to Chatelier *et al.,* (2020)[27], the surface $(2\bar{1}0)$ is a highly selective but moderately active catalyst for butadiene semi-hydrogenation, in which the surface activity and selectivity strongly depend on the surface structure.

Conclusions

In this work, we studied the surface structure of the complex compound, considered as a quasicrystal approximant, Al_5Co_2(001) of decagonal phases, obtained by the Czochralski method and analyzed its single grain crystal. Therefore, the PED experiment was performed with a constant beam energy of 350 eV and using the angular mode of analysis. The MSCD simulations indicate the model that presented the best agreement between the experimental and theoretical data and a good visual comparison between the patterns was the termination model (1×1), which consists of alternating P1 and P2 layers, and both are related by an 180° rotation. The Lattice parameter was optimized in relation to the model – 1 structure and the value that presented the lowest R_a was 7.625 Å. The non-structural parameters, such as: Debye temperature and surface potential, were optimized and applied in relation to the structure of the model corresponding to the linear combination of the terminations of models 2 (with 34%) and 4 (with 66%), corresponding to the values of θ_D = 575 K and V_0 = 4.6 eV, for which we found a reliability factor R_a of 0.182. Finally, this work is also important is the fact that, to date, this is perhaps the only work in which the study of the crystallographic structure was carried out by means of a satellite peak and not one of the main peaks of the element in question, which in our case was the Co 3p shake-up satellite.

Acknowledgements

This work was financially supported by Brazilian research agency Conselho Nacional de Desenvolvimento Científico e Tecnológico (CNPq) grant (310774/2020-9). We would like to acknowledge the Brazilian Synchrotron Light Source (LNLS).

References

1 W. Wolf, C. Bolfarini, S. Kiminami, and J. Botta, *Materials Characterization*, 2016, **122**, 76-82.

2 P. Šulhánek, M. Drienovský, I. Černičková, L. Ďuriška, R. Skaudžius, Ž. Gerhátová and M. Palcut, *Materials*, 2020, **13.14**, 3152.

3 R. Phillips, J. Zou, A. E. Carlsson, M. Widom, *Physical Review B*, 1994, **49.14**: 9322.

4 V. Raghavan, *Journal of Phase Equilibria and Diffusion*, 2008, **29.3**: 267-269.

5 M. Meier, J. Ledieu, M. De Weerd, Y. Huang, G. Abreu, K. Pussi, R. Diehl, T. Mazet, V. Fournée and E. Gaudry, *Physical Review B*, 2015, **91**, 085414.

6 A. Ormeci and Y. Grin, *Israel Journal of Chemistry*, 2011, **51**, 1349–1354.

7 U. Burkhardt, M. Ellner, Y. Grin and B. Baumgartner*, Powder Diffraction*, 1998, **13**, 159–162.

8 A. Bradley and C. Cheng, *Zeitschrift für Kristallographie-Crystalline Materials*, 1938, **99**, 480–487.

9 C. Chatelier, Y. Garreau, L. Piccolo, A. Vlad, A. Resta, J. Ledieu, V. Fournée, M.-C. d. Weerd, F.-E. Picca, M. De Boissieu et al., *The Journal of Physical Chemistry C*, 2020, **124**, 4552–4562.

10 Y. Chen, F. G. De Abajo, A. Chassé, R. Ynzunza, A. Kaduwela, M. Van Hove and C. Fadley, *Physical Review B*, 1998, **58**, 13121.

11 J. Cezar, P. Fonseca, G. Rodrigues, A. de Castro, R. Neuenschwander, F. Rodrigues, B. Meyer, L. Ribeiro, A. Moreira, J. Piton, M. Raulik, M. Donadio, R. Seraphim, M. Barbosa, A. De Siervo, R. Landers and A. De Brito, *Journal of Physics: Conference Series*, 2013. **425**. 072015.

12 L. De Lima, A. De Siervo, R. Landers, G. A. Viana, A. M. B. Goncalves, R. G. Lacerda, and P. Häberle, *Physical Review B*, 2013, **87**, 081403(R).

13 M. Viana, R. D. Muino, E. Soares, M. Van Hove and V. De Carvalho, *Journal of Physics: Condensed Matter*, 2007, **19**, 446002.

14 A. de Siervo, E. Soares, R. Landers, T. Fazan, J. Morais, and G. Kleiman, *Surface Science*, 2002, **504**, 215-222.

15 A. Pancotti, N. Barrett, L. Zagonel, G. Vanacore. *Journal of Applied Physics*, 2009, **106.3**: 034104.

16 L. Barreto, L. H. de Lima, D. C. Martins, C. Silva, R. C. D. C. Ferreira, R. Landers, A. de Siervo. *arXiv preprint arXiv:2008.06960*, 2020.

17 A. Pancotti, J. J. Silva, A. de Siervo, et al., Surface Science, 2021, **715**, 121937.

18 A. S. Kilian, G. J. P. Abreu, A. de Siervo, R. Landers, J. Morais, *CrystEngComm*, 2022, **24.12**: 2270-2279.

19 A. Pancotti, G. J. P. Abreu, J. L. Wang, A. V. M. Ferreira, R. Landers, A. de Siervo, *CrystEngComm*, 2017, **19.15**: 2089-2095.

20 Y. Chen, F. De Abajo, A. Chassé, R. Ynzunza, A. Kaduwela, M. A. Van Hove and C. Fadley, *Physical Review B*, 1998, **58**, 13121.

21 G. Abreu, A. Pancotti, L. De Lima, R. Landers and A. De Siervo*, Journal of nanoparticle research*, 2013, **15**, 1–10.

22 M. Van Hove, W. Moritz, H. Over, P. Rous, A. Wander, A. Barbieri, N. Materer, U. Starke, and G. Somorjai, *Surface Science Reports*, 1993, **19**, 191.

23 S. Verdier, L. El Ouatani, R. Dedryvère, F. Bonhomme, P. Biensan and D. Gonbeau, *Journal of The Electrochemical Society*, 2007, **154**, A1088–A1099.

24 D. Frost, C. McDowell, and I. Woolsey, *Molecular Physics*, 1974, vol. **27.6**, 1473–1489.

25 S. Alarcón, J. Dubois and E. Gaudry, *Philosophical Magazine*, 2011, **91**, 2894.

26 M. Meier, J. Ledieu, M.-C. De Weerd, V. Fournée and E. Gaudry, *Physical Review B*, 2016, **93**, 075412.

27 C. Chatelier, Y. Garreau, L. Piccolo, A. Vlad, A. Resta, J. Ledieu, V. Fournée, M.-C. d. Weerd, F.-E. Picca, M. De Boissieu et al., *The Journal of Physical Chemistry C*, 2020, **124**, 4552–4562.